

**CLASSICAL PROBLEMS OF LINEAR ACOUSTICS
AND WAVE THEORY**

**Transmission Loss Analysis in an Infinite Tube
with Multiple Discontinuities**

B. Tiryakioglu*

Department of Applied Mathematics, Faculty of Arts and Sciences, Marmara University, Istanbul, TR-34722 Turkey

**e-mail: burhan.tiryakioglu@marmara.edu.tr*

Received March 3, 2021; revised February 17, 2023; accepted March 16, 2023

Abstract—The effect of perforated screens and absorbing linings on the sound propagation is investigated using Mode Matching technique. This method is applied for the prediction of transmission loss (dB) for different parameter values of the geometry. Both low and high porosity are considered for perforated screens. In order to show the effect of the tube radius, length of the partial lined part and perforated screen porosities on the propagation phenomenon, graphics are plotted. The results demonstrate the significance of the parameters of the problem in the predictions for transmission loss (dB).

Keywords: transmission loss, infinite tube, perforated screen, mode matching

DOI: 10.1134/S1063771023600262

INTRODUCTION

Propagation of the sound through the waveguide has been an important research topic for physicists, applied mathematicians and engineers. However, it is a fact that some unwanted noise is produced during the propagation of the sound. This reality leads us to research and develop the physical properties of waveguides. For this reason, the physical changes of these ducts or tubes have an important place in the studies as they affect the sound propagation. In these studies, lining the duct walls with absorbing materials, adding expansion chambers or perforated structures are discussed. Especially studies on acoustic absorbing linings [1–5] and expansion chambers [6–10] have been examined in detail in the literature. Perforated structures, which have proven to be very effective, are an important research area affecting sound propagation [11–14].

In the literature, the best suitable method for propagation problems is the Wiener–Hopf technique [15, 16]. This technique can be applied to both finite, semi-infinite and infinite geometries. However, when the discontinuities in the problem increase, the application of the Wiener–Hopf technique can be difficult, as the solution becomes more complex. The Mode Matching technique [14], on the other hand, is a simple and effective method to apply, even if it cannot be applied to every geometry. Especially in infinite ducts/tubes, when there are multiple discontinuities, it is very effective compared to Wiener–Hopf technique.

The difference between the present paper and the previous one [14] is that the entire duct is coated with three different linings and it contains two perforated screens. Perforated screens in particular both make the present problem more interesting and provide transmission loss. In addition, since the duct is completely lined, the incident wave is considered to provide the boundary condition [1]. One of our aims in this study is to find the effects of different perforated screens on transmission loss. Finally, the results obtained in this study are compared with the previous study and it is graphically shown that the results are consistent.

FORMULATION OF THE PROBLEM

Consider an infinite tube which consists of three different absorbing linings and two perforated screens. The walls of the tube are assumed to be infinitely thin. Take into account the incident field propagating along a waveguide, as sketched in Fig. 1, given by [1]

$$\Psi_i(r, z) = A_0 J_0(\gamma_n r/a) e^{i\alpha_n z}, \quad (1)$$

where γ_n is the root of the equation

$$ika J_0(\gamma_n)/Z_1 + \gamma_n J_1(\gamma_n) = 0, \quad n = 1, 2, \dots \quad (2)$$

and α_n stands for

$$\alpha_n = \sqrt{k^2 - (\gamma_n/a)^2}. \quad (3)$$

Here, A_0 stands for the amplitude of the incident wave which will be taken equal to 1 in the analysis. Because of the symmetry of the geometry of the problem and of

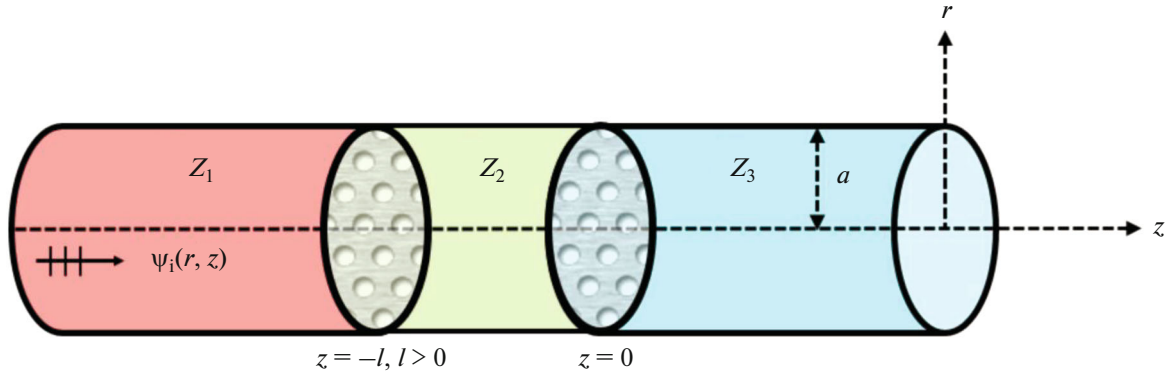


Fig. 1. Geometry of the problem.

the incident wave, the total field is independent of ϕ . Thus, the circular coordinate system is taken as (r, z) . We shall therefore introduce a scalar potential $\psi(r, z)$ which defines the acoustic pressure and velocity by $p = i\omega\rho_0\psi$ and $v = \text{grad}\psi$, respectively, where ρ_0 is the density of undisturbed medium. Throughout this study, the time dependence $\exp(-i\omega t)$ is assumed and suppressed, where ω is the angular frequency.

The total field can be written as follows

$$\psi^T(r, z) = \begin{cases} \psi_1(r, z) + \psi_i(r, z); & r < a; z \in (-\infty, -l), \\ \psi_2(r, z); & r < a; z \in (-l, 0), \\ \psi_3(r, z); & r < a; z \in (0, \infty), \end{cases} \quad (4)$$

where $\psi_1(r, z)$, $\psi_2(r, z)$ and $\psi_3(r, z)$ denote the unknown fields to be determined. These field terms are determined by the below boundary conditions:

$$\left(\frac{ik}{Z_1} - \frac{\partial}{\partial r}\right)\psi_1(a, z) = 0, \quad -\infty < z < -l, \quad (5)$$

$$\left(\frac{ik}{Z_2} - \frac{\partial}{\partial r}\right)\psi_2(a, z) = 0, \quad -l < z < 0, \quad (6)$$

$$\left(\frac{ik}{Z_3} - \frac{\partial}{\partial r}\right)\psi_3(a, z) = 0, \quad 0 < z < \infty. \quad (7)$$

Besides the boundary conditions given by (5)–(7), the following edge conditions should be written for the uniqueness of the solution of the problem. These conditions are as follows [17]:

$$u^T(\rho, z) = O(1), \quad z \rightarrow 0, \quad (8)$$

$$\frac{\partial}{\partial \rho} u^T(\rho, z) = O(z^{-1/2}), \quad z \rightarrow 0, \quad (9)$$

$$u^T(\rho, z) = O(1), \quad z \rightarrow -l, \quad (10)$$

$$\frac{\partial}{\partial \rho} u^T(\rho, z) = O((z+l)^{-1/2}), \quad z \rightarrow -l. \quad (11)$$

MODE MATCHING TECHNIQUE

The Mode Matching technique is a very efficient method used in many acoustic and electromagnetic problems. By using this technique, one can easily obtain the sound propagation in waveguides. Eigenmodes of each region are found and matched at each junction discontinuity to satisfy the relevant boundary conditions in Mode Matching technique [13]. The Mode Matching technique is applied to each region separately. Different series expansions are obtained according to the fact that these regions are finite-infinite and rigid-lined. These regions are $\{-\infty < z < -l\}$, $\{-l < z < 0\}$ and $\{0 < z < \infty\}$. The solutions in these regions are as follows, respectively [14]:

$$\psi_1(r, z) = \sum_{n=1}^{\infty} R_n e^{-i\alpha_n z} J_0(\gamma_n r/a), \quad (12)$$

$$\psi_2(r, z) = \sum_{n=1}^{\infty} [A_n e^{i\chi_n z} + B_n e^{-i\chi_n z}] J_0(\tau_n r/a), \quad (13)$$

$$\psi_3(r, z) = \sum_{n=1}^{\infty} T_n e^{i\beta_n z} J_0(\xi_n r/a), \quad (14)$$

where τ_n and ξ_n are the roots of the following equations respectively

$$ikaJ_0(\tau_n)/Z_2 + \tau_n J_1(\tau_n) = 0, \quad n = 1, 2, \dots, \quad (15)$$

$$ikaJ_0(\xi_n)/Z_3 + \xi_n J_a(\xi_n) = 0, \quad n = 1, 2, \dots \quad (16)$$

and χ_n, β_n stand for

$$\chi_n = \sqrt{k^2 - (\tau_n/a)^2}, \quad (17)$$

$$\beta_n = \sqrt{k^2 - (\xi_n/a)^2}. \quad (18)$$

Here, R_n and T_n are the amplitude of the reflected and transmitted mode in relevant regions, respectively. From the geometry of the problem, the following continuity conditions can be written easily

$$\frac{\partial}{\partial z} \psi_2(r, -l) = \frac{\partial}{\partial z} \psi_1(r, -l) + \frac{\partial}{\partial z} \psi_i(r, -l), \quad (19)$$

$$\psi_2(r, -l) + i \frac{\zeta_p^1}{k} \frac{\partial}{\partial z} \psi_2(r, -l) = \psi_1(r, -l) + \psi_i(r, -l), \quad (20)$$

$$\frac{\partial}{\partial z} \psi_2(r, 0) = \frac{\partial}{\partial z} \psi_3(r, 0), \quad (21)$$

$$\psi_2(r, 0) = \psi_3(r, 0) + i \frac{\zeta_p^2}{k} \frac{\partial}{\partial z} \psi_3(r, 0). \quad (22)$$

Here, $\zeta_p^{1,2}$ are the specific impedance, describing the acoustic properties of the perforated screen. For stationary media, the empirical formula of the specific acoustic impedance $\zeta_p^{1,2}$ are given by [11] as

$$\zeta_p^1 = [0.006 - ik(t_w^1 + 0.75d_h^1)]/\sigma_1, \quad (23)$$

$$\zeta_p^2 = [0.006 - ik(t_w^2 + 0.75d_h^2)]/\sigma_2, \quad (24)$$

where $t_w^{1,2}$ is the screen thickness, $d_h^{1,2}$ is the perforate hole diameter and $\sigma_{1,2}$ the porosity. Eqs. (19) and (20) can be written from the continuity relations at the point $-l$ and (21), (22) are obtained by the continuity relations at the point 0. Using the Mode Matching technique at the point $z = -l$, we obtain the following equations

$$\begin{aligned} & i \sum_{n=1}^{\infty} \chi_n [A_n e^{-i\chi_n l} - B_n e^{i\chi_n l}] J_0(\tau_n r/a) \\ &= -i \sum_{m=1}^{\infty} \alpha_m R_m e^{i\alpha_m l} J_0(\gamma_m r/a) + i A_0 J_0(\gamma_s r/a) e^{-i\alpha_s l}, \end{aligned} \quad (25)$$

$$\begin{aligned} & \sum_{n=1}^{\infty} [A_n (1 - \zeta_p^1 \chi_n/k) e^{-i\chi_n l} + B_n (1 + \zeta_p^1 \chi_n/k) e^{i\chi_n l}] J_0(\tau_n r/a) \\ &= \sum_{m=1}^{\infty} R_m e^{i\alpha_m l} J_0(\gamma_m r/a) + A_0 J_0(\gamma_s r/a) e^{-i\alpha_s l}. \end{aligned} \quad (26)$$

Similar analysis is also carried out for $z = 0$, we get

$$i \sum_{n=1}^{\infty} \chi_n [A_n - B_n] J_0(\tau_n r/a) = i \sum_{m=1}^{\infty} \beta_m T_m J_0(\xi_m r/a), \quad (27)$$

$$\begin{aligned} & \sum_{n=1}^{\infty} [A_n + B_n] J_0(\tau_n r/a) \\ &= \sum_{m=1}^{\infty} T_m (1 - \zeta_p^2 \beta_m/k) J_0(\xi_m r/a). \end{aligned} \quad (28)$$

By using the orthogonality conditions in each equation, we obtain the following systems of equations

$$\begin{aligned} & \frac{Z_1(Z_3 - Z_2)}{Z_3(Z_1 - Z_2)} \sum_{m=1}^{\infty} T_m \frac{\chi_n (1 - \zeta_p^2 \beta_m/k) + \beta_m}{\tau_n^2 - \xi_m^2} J_0(\xi_m) \\ & - \sum_{m=1}^{\infty} R_m \frac{\chi_n - (1 + \zeta_p^1 \chi_n/k) \alpha_m}{\tau_n^2 - \gamma_m^2} e^{i(\alpha_m + \chi_n)l} J_0(\gamma_m) \end{aligned} \quad (29)$$

$$= A_0 \frac{J_0(\gamma_s)}{\tau_n^2 - \gamma_s^2} [\chi_n + (1 + \zeta_p^1 \chi_n/k) \alpha_s] e^{i(\chi_n - \alpha_s)l},$$

$$\begin{aligned} & \frac{Z_1(Z_3 - Z_2)}{Z_3(Z_1 - Z_2)} \sum_{m=1}^{\infty} T_m \frac{\chi_n (1 - \zeta_p^2 \beta_m/k) - \beta_m}{\tau_n^2 - \xi_m^2} J_0(\xi_m) \\ & - \sum_{m=1}^{\infty} R_m \frac{\chi_n + (1 - \zeta_p^1 \chi_n/k) \alpha_m}{\tau_n^2 - \gamma_m^2} e^{i(\alpha_m + \chi_n)l} J_0(\gamma_m) \end{aligned} \quad (30)$$

$$= A_0 \frac{J_0(\gamma_s)}{\tau_n^2 - \gamma_s^2} [\chi_n - (1 - \zeta_p^1 \chi_n/k) \alpha_s] e^{-i(\chi_n + \alpha_s)l}.$$

The unknown coefficients R_m and T_m can be determined by using the linear systems of equations (29) and (30). Since the infinite series converge rapidly they can be truncated at a certain point. So, all the numerical results will be derived by truncating the infinite series and the infinite systems of linear algebraic equations after the first N terms.

NUMERICAL RESULTS

Graphics are presented for the analysis of tube radius, length of Z_2 lining, porosities of two different perforated screens, etc. In these graphs, the effects of parameter values on transmission loss (TL) are examined. In this study, parameter values such as tube radius, lining length of Z_2 are used by making use of some studies in the literature [13, 18]. For the comparison graph, the previous study is analyzed [14]. Transmission loss (TL) is calculated numerically with the expression given below

$$TL = -20 \log_{10} |T_1|.$$

Figure 2 shows the variation of the transmission loss (dB) amplitude with the truncation number N . It is seen that the amplitude of the transmission loss (dB) becomes insensitive to the increase of the truncation number after $N = 5$ for $Z_1 = 1 + 3i$, $Z_2 = 1 - li$ and $Z_3 = 1 - 3i$.

Figure 3 shows the transmission loss (dB) results for different waveguide radii a . In Fig. 3, one can see that the amplitude of the transmission loss (dB) decreases with increasing values of a .

Similar analysis is also carried out for Fig. 4 which displays the effect of lining length Z_2 to the transmission loss (dB). In Fig. 4, the amplitude of the transmission loss (dB) increases with the increasing value of lining length Z_2 , as expected.

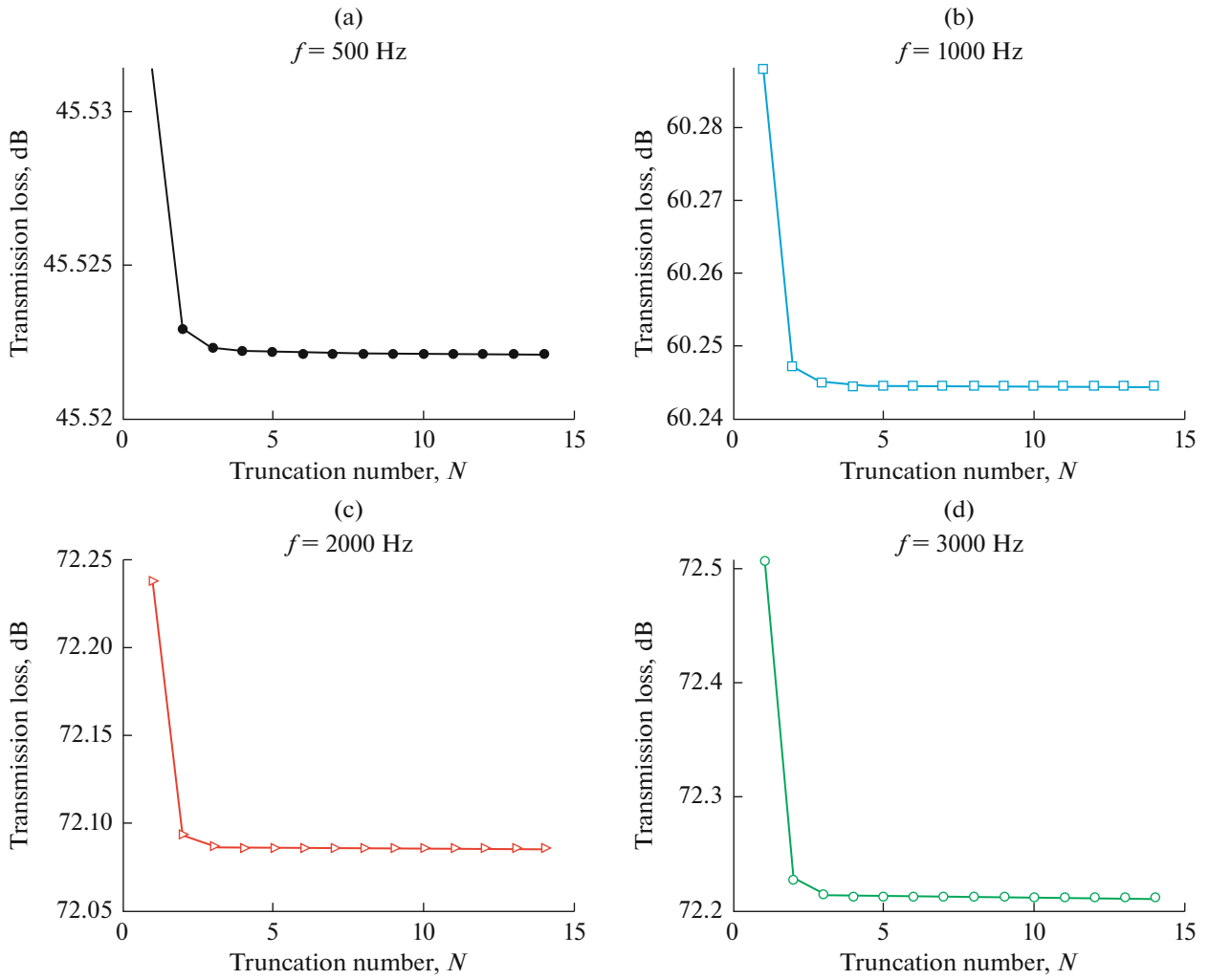


Fig. 2. Amplitude of the transmission loss (dB) versus the truncation number N with $a = 0.015$ m, $l = 0.25$ m, $Z_1 = 1 + 3i$, $Z_2 = 1 - li$, $Z_3 = 1 - 3i$, $t_w^{1,2} = 0.0009$ m, $d_h^{1,2} = 0.00249$ m and $\sigma_{1,2} = 8.4\%$.

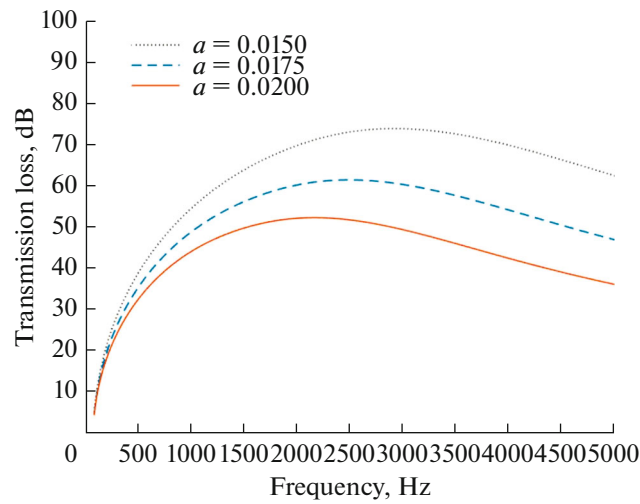


Fig. 3. Transmission loss versus the tube radius with $l = 0.25$ m, $Z_1 = 1 + 3i$, $Z_2 = 1 - li$, $Z_3 = 1 - 3i$, $t_w^{1,2} = 0.0009$ m, $d_h^{1,2} = 0.00249$ m and $\sigma_{1,2} = 8.4\%$.

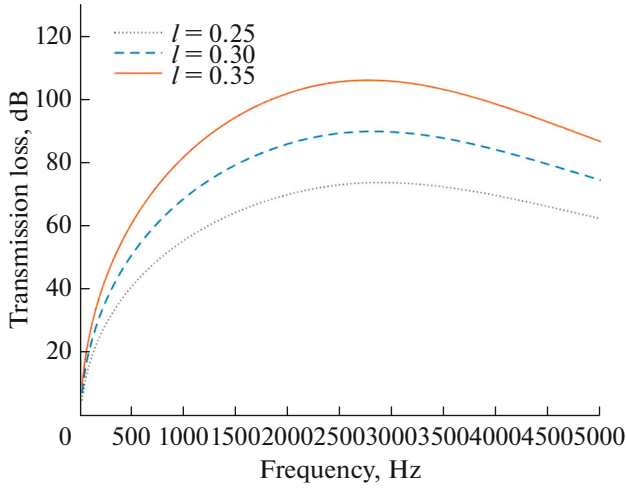


Fig. 4. Transmission loss versus the lining length of Z_2 with $a = 0.015$ m, $Z_1 = 1 + 3i$, $Z_2 = 1 - li$, $Z_3 = 1 - 3i$, $t_w^{1,2} = 0.0009$ m, $d_h^{1,2} = 0.00249$ m and $\sigma_{1,2} = 8.4\%$.

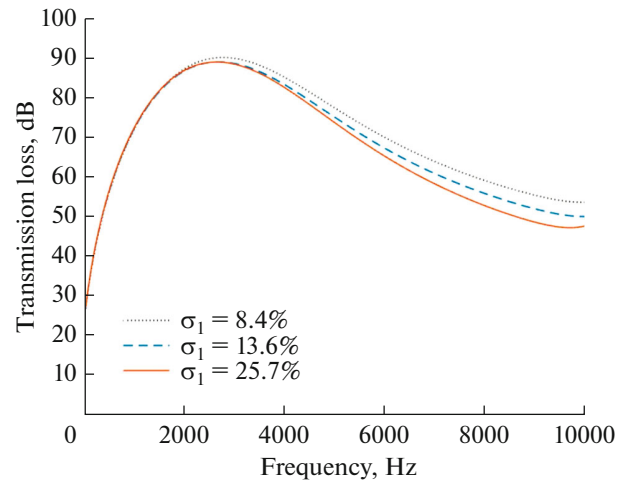


Fig. 5. Transmission loss versus the porosity (σ_1) with $a = 0.015$ m, $l = 0.25$ m, $Z_1 \rightarrow \infty$, $Z_2 = 1 - li$, $Z_3 \rightarrow \infty$, $t_w^{1,2} = 0.0009$ m, $d_h^{1,2} = 0.00249$ m and $\sigma_2 = 25.7\%$.

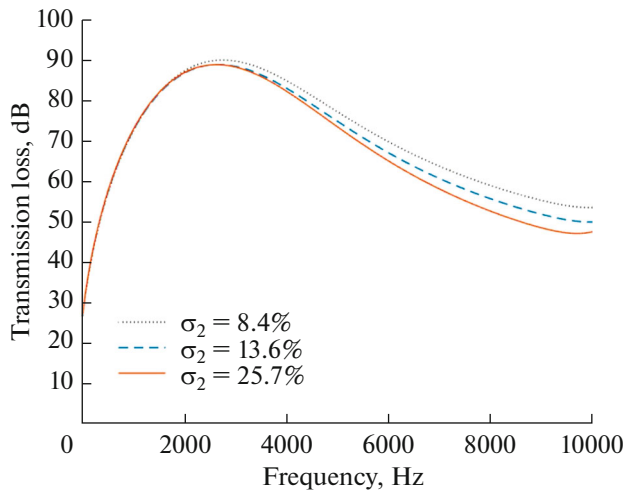


Fig. 6. Transmission loss versus the porosity (σ_2) with $a = 0.015$ m, $l = 0.25$ m, $Z_1 \rightarrow \infty$, $Z_2 = 1 - li$, $Z_3 \rightarrow \infty$, $t_w^{1,2} = 0.0009$ m, $d_h^{1,2} = 0.00249$ m and $\sigma_1 = 25.7\%$.

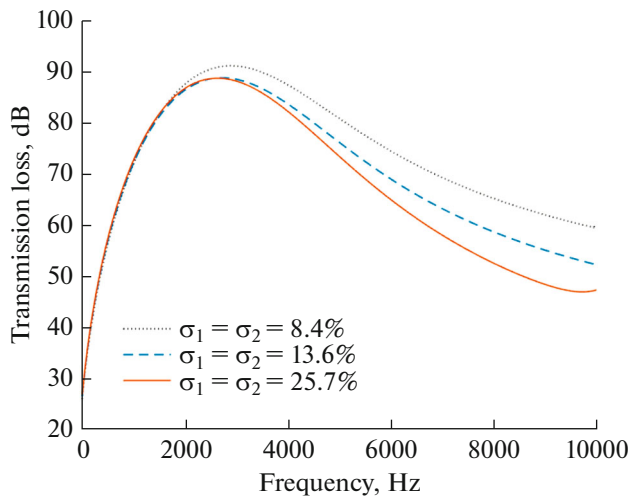


Fig. 7. Transmission loss versus the porosity ($\sigma_{1,2}$) with $a = 0.015$ m, $l = 0.25$ m, $Z_1 \rightarrow \infty$, $Z_2 = 1 - li$, $Z_3 \rightarrow \infty$, $t_w^{1,2} = 0.0009$ m and $d_h^{1,2} = 0.00249$ m.

Figures 5, 6 and 7 show the transmission loss (dB) of the infinite lined tube with different screen porosities. The porosity parameters in Eqs. (19)–(20) are changed while the other quantities are kept as in the previous cases. These porosities are taken as 8.4, 13.8 and 25.7%. It is observed that there are similar behaviors up to a certain frequency in all three graphs. While the perforations do not affect the transmission loss (dB) up to a certain frequency, lower porosity increases the transmission loss (dB) after approximately 3000 Hz. It can be seen that the amplitude of

the transmission loss (dB) in the Fig. 7 is more than the amplitudes in the Figs. 5 and 6. Since both σ_1 and σ_2 change at the same time, a larger amplitude difference occurs.

Figure 8 depicts an excellent agreement between the present paper and previous study [14]. For the comparison graph in Fig. 8, the parameter values are changed and transmission loss (dB) is plotted. This graphic is important in terms of showing that the complicated problem is solved correctly and that different methods can be applied to the same problem [14].

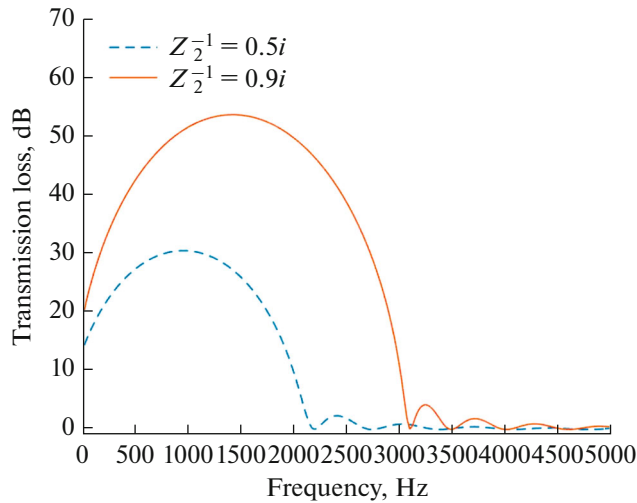


Fig. 8. Comparison of the transmission loss with the study of [14] for $a = 0.0243\text{m}$, $l = 0.21981\text{ m}$, $Z_1 \rightarrow \infty$, $Z_3 \rightarrow \infty$ and $\zeta_p^{1,2} \rightarrow 0$.

CONCLUSION

A rigorous investigation is presented for the problem of propagation of sound waves from an infinite tube with multiple discontinuities. The Mode Matching technique is used to obtain transmission loss (dB). The tube is assumed to be lined with three different absorbing linings and includes two different perforated screens. The solution consisting of complex equation systems is calculated numerically. Using this solution, graphs are produced for different parameters. In addition, it is observed that it is possible to increase the transmission loss (dB) by changing the tube parameters and perforated screen porosities. The accuracy of the results obtained in this study is compared with the previous study. The result is excellent.

CONFLICT OF INTEREST

The authors declare that they have no conflicts of interest.

REFERENCES

1. A. D. Rawlins, Proc. R. Soc. London A **361**, 65 (1978).
2. A. F. Sobolev and M. A. Yakovets, Acoust. Phys. **63**, 625 (2017).
3. M. H. Tiwana, R. Nawaz, and A. B. Mann, Anal. Math. Phys. **7** (4), 525 (2017).
4. B. Tiryakioglu, Int. J. Aeroacoust. **19** (1–2), 38 (2020).
5. N. Peake and I. D. Abrahams, Wave Motion **92**, 102407 (2020).
6. A. Selamet and Z. L. Ji, J. Sound Vib. **223** (2), 197 (1999).
7. A. Demir and A. Buyukaksoy, Int. J. Eng. Sci. **41** (20), 2411 (2003).
8. A. Selamet, M. B. Xu, and I. J. Lee, Int. J. Vehicle Noise Vib. **1**, 341 (2005).
9. A. Demir and A. Buyukaksoy, Int. J. Eng. Sci. **43** (5), 398 (2005).
10. Z. Fang and C. Y. Liu, Eng. Anal. Bound Elem. **84**, 168 (2017).
11. J. W. Sullivan and M. J. Crocker, J. Acoust. Soc. Am. **64**, 207 (1978).
12. C. Lawn, Appl. Acoust. **89**, 211 (2015).
13. B. Tiryakioglu, J. Eng. Math. **122** (1), 17 (2020).
14. B. Tiryakioglu, Acoust. Phys. **66** (6), 580 (2020).
15. B. Noble, *Methods Based on the Wiener-Hopf Techniques* (London, 1958).
16. J. B. Lawrie and I. D. Abrahams, J. Eng. Math. **59** (4), 351 (2007).
17. R. Mittra and S. W. Lee, *Analytical Techniques in the Theory of Guided Waves* (Macmillan Co., 1971).
18. I. Lee, A. Selamet, and N. T. Huff, J. Acoust. Soc. Am. **120**, 3706 (2006).